JOURNAL OF APPLIED ELECTROCHEMISTRY **23** (1993) 915–921

Hydrogen evolution reaction (h.e.r.) in an acidic or basic medium on nickel electrodeposited with $PW_{12}O_{40}^{3-}$ and Cu^{2+}

O. SAVADOGO*, E. NDZEBET

Département de métallurgie et de Génie des Matériaux, Ecole Polytechnique de Montréal, C.P. 6079, succ. "A" Montréal (QC), H3C3A7 Canada

Received 9 December 1991; revised 24 November 1992

The hydrogen evolution reaction (h.e.r.) on electrodeposited nickel from a chemical bath containing Cu^{2+}, with and without $PW_{12}O_{40}^{3-}$, was investigated. Hydrogen cathodes based on nickel–copper alloys and $PW_{12}O_{40}^{3-}$ reduced species are better electrocatalysts in 1 M H_2SO_4 or 3 M KOH at 298 K than nickel–copper alloys deposited without $PW_{12}O_{40}^{3-}$. The electrocatalytic performance of the former cathodes was attributed to their chemical composition. This electrocatalytic activity for the h.e.r. was examined as a function of the $[Cu^{2+}]$ or $[PW_{12}O_{40}^{3-}]$ in the electrodeposition bath. The influence of nickel salt anions on the h.e.r. electrocatalytic activity of the electrodes was also investigated. The chemical surface composition of the electrodes was analysed by X-ray photoelectron spectroscopy (XPS). It was shown that the electrocatalytic parameters were correlated to the quantity of tungsten in the electrode surface. The various factors causing the improvement in the electrocatalytic activity are discussed.

---

1. Introduction

Recently, there has been considerable interest in the development of new electrode materials with sufficient electrocatalytic activity for various electrochemical processes. The study of the hydrogen evolution reaction (h.e.r.) on electromodified electrodes has been summarized elsewhere [1, 2]. Typical issues arising from the electrocatalytic activity achieved as a function of the combination of hypo-hyper-d-electronic transition metals have been presented [3]. Based on the concepts of the Brewer theory of intermetallic phases [4–6], it has been shown that the bulk properties of these intermetallic phases determine their electrocatalytic activity for the h.e.r. This reaction has also been performed on chevrel-type cluster compounds [7]. The remixed cluster compounds were found to be the most highly efficient electrodes for the h.e.r. (both intermetallic systems of hypo-hyper-d-electronic metal combinations and cluster materials were prepared thermally). It has already been demonstrated that the electrocatalytic activity of electrodeposited nickel electrodes with heteropolyacids (HPAs) for the h.e.r. is far superior to that of electrodeposited nickel electrodes without HPAs [8–11]. It has also been found recently that the incorporation of Cu^{2+} ions in the electrolyte significantly improves the electrocatalytic activity of electrodes surface-modified with HPA for the h.e.r. in a basic medium [12].

This paper deals with electrocatalytic behaviour for the h.e.r. in 1 M H_2SO_4 or 3 M KOH on electrodeposited nickel with Cu^{2+} and $PW_{12}O_{40}^{3-}$. The influence of $[Cu^{2+}]$ and $[PW_{12}O_{40}^{3-}]$ in the electrodeposition bath on the electrocatalytic activity of these electrodes was examined. This electrocatalytic activity was also studied as a function of the nickel salt anions used in the bath. The nickel electrodes deposited with Cu^{2+} and without $PW_{12}O_{40}^{3-}$ were labelled Ni(Cu), while those deposited with Cu^{2+} and $PW_{12}O_{40}^{3-}$ were labelled $NiCu(PW_{12})10^{-x}$ (10^{-x} is the molar concentration of $PW_{12}O_{40}^{3-}$). Finally, nickel electrodes deposited with $PW_{12}O_{40}^{3-}$ and without Cu^{2+} were labelled $Ni(PW_{12})10^{-x}$.

2. Experimental procedure

2.1. *Electrodeposition*

The electrodeposition of nickel was carried out mainly from a chloride bath consisting of: 0.25 M $NiCl_2.6H_2O$; 1 M H_3BO_3; 0.12 M HCl and 1.0×10^{-4} M sodium dodecyl sulphate. To investigate the influence of nickel salt anions on the electrocatalytic activity of the electrodeposits, acetate and sulphate baths were also used. The chemical composition of the acetate bath was: 0.25 M $Ni(CH_3COO)_2.4H_2O$; 1 M H_3BO_3; 0.23 M CH_3COONH_4; 7.0×10^{-2} M CH_3COONa; 1.0×10^{-4} M sodium dodecyl sulphate and 7.0×10^{-2} M Na_2SO_4, while that of the sulfate was 0.25 M $NiSO_4.6H_2O$; 1 M H_3BO_3; 0.14 M Na_2SO_4; 0.3 M $(NH_4)_2SO_4$; and 1.0×10^{-4} M sodium dodecyl

---

* To whom correspondence should be sent.

0021-891X

sulphate (all of reagent grade). Double-distilled water was used in preparing the solution. The substrate was 316 stainless steel (Firth Brown Inox) with an 8 cm^2 surface area. During electrodeposition, two sheets of nickel (99.9% grade, Sargent Welch) 0.8 mm thick, both with a surface area of 9 cm^2, were used as the anodes. Prior to electrodeposition, the electrodes were first degreased with acetone and then treated with 60% HNO_3 for 5 min. Finally, the electrodes were thoroughly washed with double-distilled water. They were then activated by anodic electrochemical polishing for 20 min in 1 M H_2SO_4 at a current density of 35 mA cm^{-2} using a Hewlett Packard power supply (model HP6266B). The electrodeposition of nickel was performed from a chemical bath containing different concentrations of Cu^{2+} and $PW_{12}O_{40}^{3-}$ at a current density of 35 mA cm^{-2} using the same power supply. The electrodeposition process lasted 6 h, and the temperature was maintained at 55 ± 5 °C. The reproducibility of this process was checked at least ten times for each electrode and the results were found to be quite reproducible at a rate of 90%.

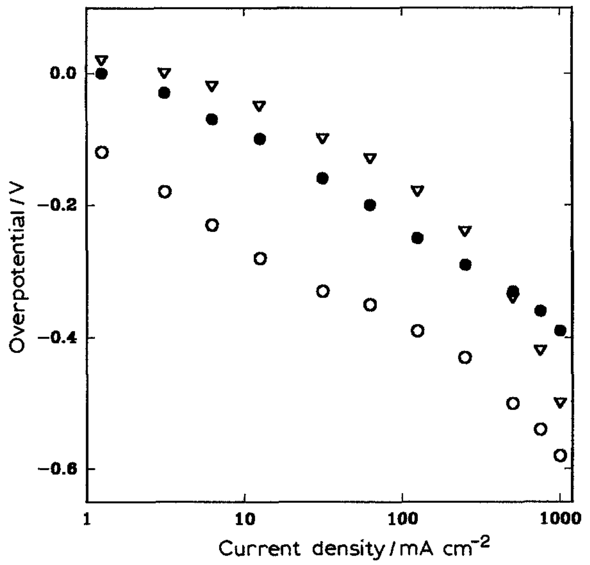

Fig. 1. Cathodic polarization curves for the h.e.r. under galvanostatic conditions in 1 M H_2SO_4 at 298 K on nickel electrodeposited with various concentrations of Cu^{2+} and 1.0×10^{-4} M of $PW_{12}O_{40}^{3-}$: (○) without Cu^{2+}; (●) with 1.0×10^{-5} M Cu^{2+}; and (△) with 6.4×10^{-4} M Cu^{2+}.

2.2 BET surface measurement

Classical static-type BET measurements were carried out with Flowsorb 112300 equipment using a monolithic cell, through which flow liquid nitrogen and a standard mixture of 0.1% krypton in helium.

2.3. Electrochemical equipment and electrodes

All the electrochemical measurements were carried out in a single-compartment cell with a three-electrode configuration at room temperature (298 K) using a Hewlett Packard power supply (model HP 6266 B). The electrode potential was measured and referred to a saturated calomel electrode (SCE). A platinum gauze electrode with a large surface area was used as a counter electrode (CE). The working electrode (WE) was the electrodeposited nickel with a geometrical surface area of 8 cm^2. All experimental results were referred to this apparent geometric area, which possibly differed to some extent from the real surface area of the samples [12–14]. A discussion of electrocatalytic activity based on the real surface area was therefore considered, following BET surface determination. The electrolyte was thoroughly deoxygenated with pure nitrogen gas, and kept under positive pressure of this gas during the experiment. The XPS analyses were carried out using a vacuum generator, the ESCLAB MKII ESCA/AUGER spectrophotometer with 280 W of power, 14 kV ($E = 1253.6$ eV). All the binding energies reported were referenced to C 1s at 285 eV. The survey and multiplex spectra, which were measured after the data had been smoothed, are reported as obtained.

3. Results and discussion

3.1. Results obtained in 1 M H_2SO_4 solution

Figure 1 shows the iR-corrected cathodic polarization curves obtained on electrodeposited nickel with different concentrations of Cu^{2+} and 1.0×10^{-4} M of $PW_{12}O_{40}^{3-}$ from a chloride bath. All these polarization curves exhibit typical Tafel behaviour over a large potential domain for the h.e.r. Therefore, the h.e.r. electrocatalytic parameters, such as the hydrogen overpotential (η), exchange current density (i_o) and the Tafel slope (b), can be deduced from these curves.

The variation of these parameters with different concentrations of Cu^{2+} are presented in Table 1. As may be seen, the $NiCu(PW_{12})10^{-4}$ electrodes exhibited higher exchange current density (i_o) and lower overpotential (η) than those of $Ni(PW_{12})10^{-4}$. On the other hand, both the $Ni(PW_{12})10^{-4}$ and $NiCu(PW_{12})10^{-4}$ electrodes exhibited the same Tafel slope (130 ± 10 mV dec^{-1}). From these results, it may be concluded that $NiCu(PW_{12})10^{-4}$ electrodes are more electrocatalytic for the h.e.r. than

Table 1. The hydrogen overvoltage (η) at -500 mA cm^{-2}, the h.e.r. exchange current density (i_o) and the Tafel slope (b) in 1 M H_2SO_4 on electrodeposited nickel with different concentrations of Cu^{2+} with 1.0×10^{-4} M of $PW_{12}O_{40}^{3-}$

$CuSO_4$/M	b/mV dec^{-1}	i_o/mA cm^{-2}	$\lvert\eta\rvert$/mV
0.0	140	0.34	450
1.0×10^{-5}	140	5.00	340
6.4×10^{-4}	130	6.00	300

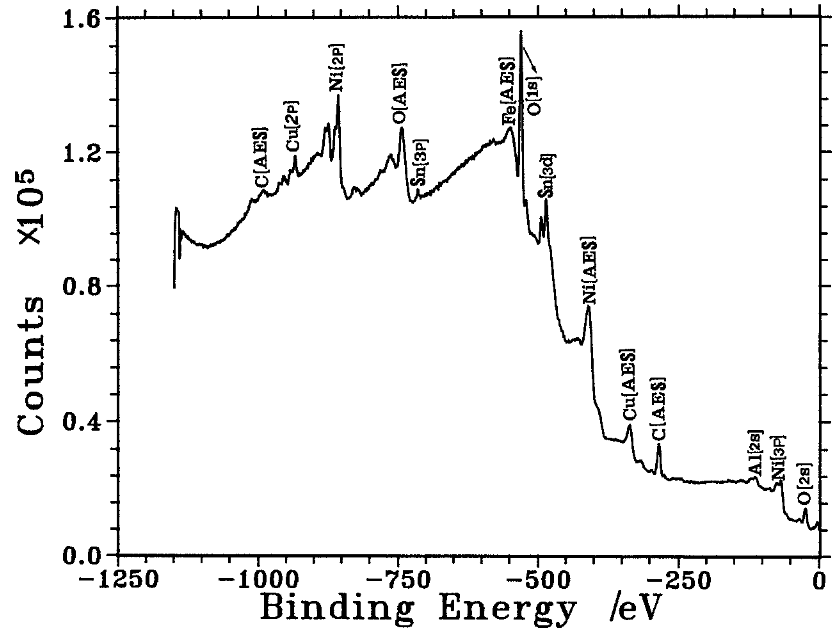

Fig. 2. XPS survey scan of the $NiCu(PW_{12})10^{-4}$ electrode showing the various elements detected on its surface.

$Ni(PW_{12})10^{-4}$ electrodes. Also, the h.e.r. electrocatalytic activity of $NiCu(PW_{12})10^{-4}$ electrodes improves significantly when $[Cu^{2+}]$ increases. The surface composition of these electrodes was determined by XPS. Figure 2 shows the XPS spectra of electrodeposited nickel with 6.4×10^{-4} M of Cu^{2+} and 1.0×10^{-4} M of $PW_{12}O_{40}^{3-}$ prior to electrochemical characterization. These spectra reveal the presence of Ni, Cu, W and other elements such as Sn, C, Al and Fe on the electrode surface. Phosphorous was not detected. After argon ion etching for a few minutes, Sn, C, Al and Fe contaminants were substantially removed. The W photoemission spectra showed two peak positions with binding energies of 37.40 ($4f_{5/2}$) and 35.4 eV ($4f_{7/2}$), respectively (see Fig. 3). Consequently, tungsten was presumably present in the form of WO_3. This result is in agreement with other published data [15]. In the case of copper, the binding energy value of 933 eV (Cu 2p) suggests that this element was probably present as CuO (see Fig. 4). The binding energy values of Ni were 862.0 and 856.7 eV (Ni 2p) for peak 1 and peak 2 respectively, indicating that the nickel is bound to several oxygen atoms (Fig. 5). It should be noted that the elements W and Ni were also detected on the $Ni(PW_{12})10^{-4}$ surface electrode. Therefore, the atomic concentrations of various elements evaluated from the XPS analysis of $Ni(PW_{12})10^{-4}$ and of nickel electrodes deposited with different concentrations of $PW_{12}O_{40}^{3-}$ and 6.4×10^{-4} M of Cu^{2+} are listed in Table 2. As may be seen, a significant increase in the atomic concentrations of Ni and W occurred between the

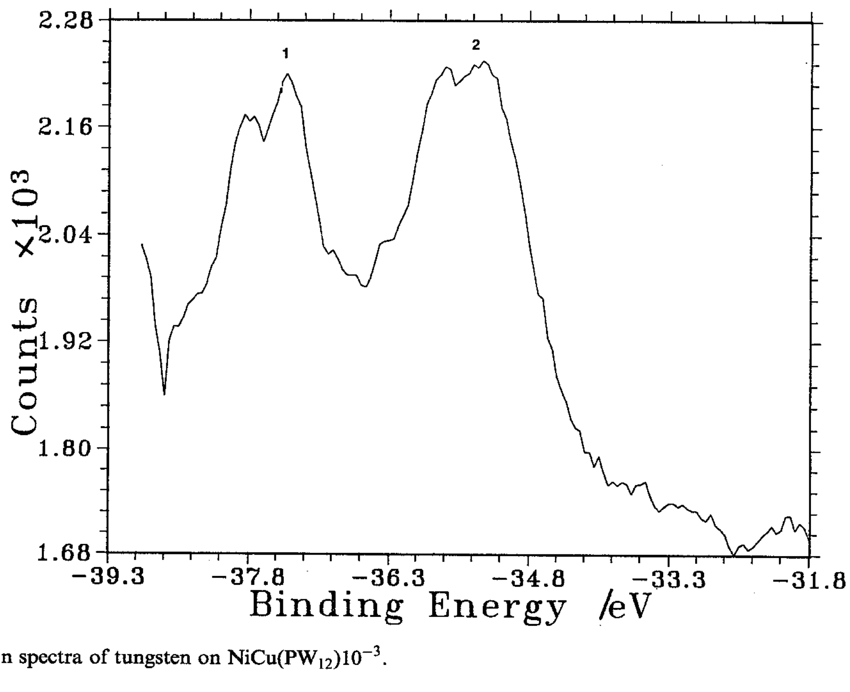

Fig. 3. Photoemission spectra of tungsten on $NiCu(PW_{12})10^{-3}$.

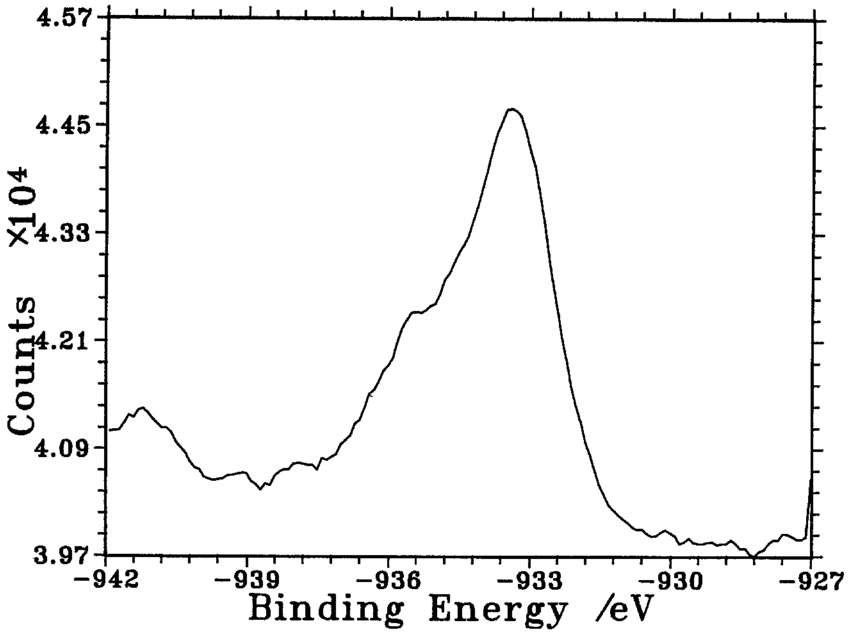

Fig. 4. Photoemission spectra of copper on $NiCu(PW_{12})10^{-3}$.

$Ni(PW_{12})10^{-4}$ and the $NiCu(PW_{12})$ electrodes. This result may be attributed to the use of Cu^{2+} ions in the electrodeposition bath. The BET surface area measurements of the $Ni(PW_{12})10^{-4}$ and $NiCu(PW_{12})10^{-4}$ electrodes showed that the real surface area of these electrodes was the same, and equal to $0.1\,m^2\,g^{-1}$. The double layer capacitance of these electrodes were also measured in a 0.5 M Na_2SO_4 solution by cyclic voltammetry. These measurements were carried out within the ideal polarization potential range (the faradaic current was negligible). The double layer capacitance varied from $0.19\,\mu F\,cm^{-2}$ on the $Ni(PW_{12})10^{-4}$ electrode to $0.22\,\mu F\,cm^{-2}$ in the case of the $NiCu(PW_{12})10^{-4}$ electrode. These electrodes therefore probably have the same electrochemically active surface area. From these experimental results, it may be concluded that the significant enhancement for the h.e.r. electrocatalytic activity observed on the $NiCu(PW_{12})10^{-4}$ electrodes is related to their chemical composition, rather than to an increase in their electrochemically active surface area or BET surface area.

The influence of $[PW_{12}O_{40}^{3-}]$ on the electrocatalytic activity of deposited nickel electrodes for the h.e.r. was also studied. The electrodes were deposited with 6.4×10^{-4} M of Cu^{2+}, and various $PW_{12}O_{40}^{3-}$ concentrations, from the chloride bath. Table 3 shows the kinetic parameters for the h.e.r. on these electrodes, evaluated from the cathodic polarization curves (Fig. 6). As may be seen, the highest i_0 and the lowest η were obtained on electrodeposited nickel with Cu^{2+}

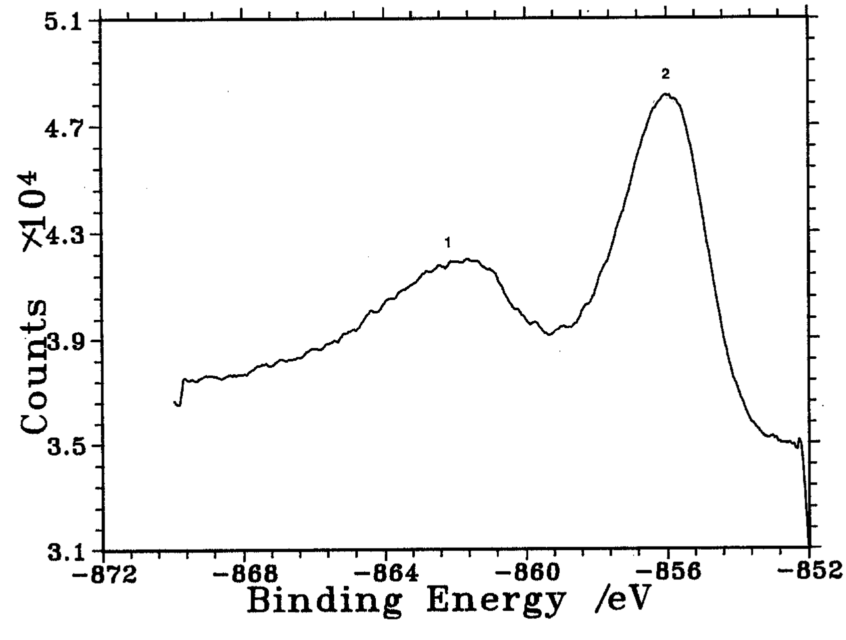

Fig. 5. Photoemission spectra of nickel on $NiCu(PW_{12})10^{-3}$.

Table 2. Atomic concentrations of the various elements determined from the XPS analysis at the (a) Ni(PW_{12})10^{-4}, (b) NiCu(PW_{12})10^{-6}, (c) NiCu(PW_{12})10^{-5}, (d) NiCu(PW_{12})10^{-4} and (e) NiCu(PW_{12})10^{-3} surface electrodes

Elements	*Atomic concentration/%* (±0.05%)				
	(a)	(b)	(c)	(d)	(e)
Ni	15.0	19.50	19.70	19.72	19.70
Cu	–	3.60	3.58	3.53	3.57
W	0.48	0.76	0.60	0.54	0.51
O	84.5	81.5	75.94	76.21	76.22

Table 3. Variation in the Tafel slope (b), the overpotential (η) at -500 mA cm^{-2} and the exchange current density (i_o) for the h.e.r. at 298 K in 1 M H_2SO_4 on electrodeposited nickel with various $PW_{12}O_{40}^{3-}$ concentrations and 6.4×10^{-4} M of Cu^{2+} from a chloride bath

($H_3PW_{12}O_{40}$)/M	b/mV dec^{-1}	i_o/mA cm^{-2}	$\|\eta\|$/mV
0.0	120	1.00	460
1.0×10^{-6}	120	12.00	290
1.0×10^{-5}	150	6.00	370
1.0×10^{-4}	130	6.00	300
1.0×10^{-3}	160	8.30	300

Table 4. Variation of the Tafel slope (b), the overpotential (η) at -500 mA cm^{-2} and the exchange current density (i_o) for the h.e.r. at 298 K in 3 M KOH on electrodeposited nickel with various $PW_{12}O_{40}^{3-}$ concentrations and 6.4×10^{-4} M of Cu^{2+} from a chloride bath

($H_3PW_{12}O_{40}$)/M	b/mV dec^{-1}	i_o/mA cm^{-2}	$\|\eta\|$/mV
0.0	100	0.03	530
1.0×10^{-6}	160	0.90	550
1.0×10^{-5}	120	0.70	550
1.0×10^{-4}	130	0.06	580
1.0×10^{-3}	190	1.10	370

and $PW_{12}O_{40}^{3-}$. On the other hand, the atomic concentrations of various elements determined from the XPS spectra of these electrodes reveal that only the tungsten atomic concentration [W] changes from one electrode surface to another, the copper atomic concentration remaining constant (see Table 2). The variation of i_o with [W] is shown in Fig. 7. It will be noted that, the maximum value of i_o is obtained for the maximum value of [W]. The lowest overpotential is also obtained for the maximum value of [W]. On the other hand, the h.e.r. Tafel slope does not change with [W] (see Tables 3 and 4). This suggests that for these electrodes a high i_o and a low η are only characteristic of a good electrocatalyst. The significant improvement in the values of i_o may be attributed to various factors: (a) the interaction between the nickel matrix, WO_3, and Cu products, weakening the strength of the Ni–H bond, and hence the energy required for the reactant to make the transition from the base state to the activated state is reduced; (b) the dispersion of WO_3 and Cu products in the nickel metal increases the number of nickel crystal dislocations and defects and, consequently, the number of reaction sites and the reaction rate; (c) the addition of WO_3 into the nickel matrix has the same effect as the addition of a catalysis promoter into a main catalyst.

3.2. Results obtained in 3 M KOH solution

The electrocatalytic activity for the h.e.r. on the electrodeposited nickel with 6.4×10^{-4} M of Cu^{2+}, with and without $PW_{12}O_{40}^{3-}$, from a chloride bath has been also investigated in 3 M KOH. As in the case of an acidic medium, the cathodic polarization curves obtained in a basic medium also show the Tafel behaviour over a large potential domain for the h.e.r. (Fig. 8). The electrocatalytic parameters for the h.e.r. determined from these cathodic polarization curves are listed in Table 4. The exchange current density of the Ni(Cu) electrode was lower than that of the nickel electrode deposited with Cu^{2+} and $PW_{12}O_{40}^{3-}$. On the other hand, the increase in [$PW_{12}O_{40}^{3-}$] was found to involve a slight increase in overpotential, except in the case of the NiCu(PW_{12})10^{-3} electrode, which exhibited a decrease in overpotential of 160 mV with respect to that of Ni(Cu) at a current density of

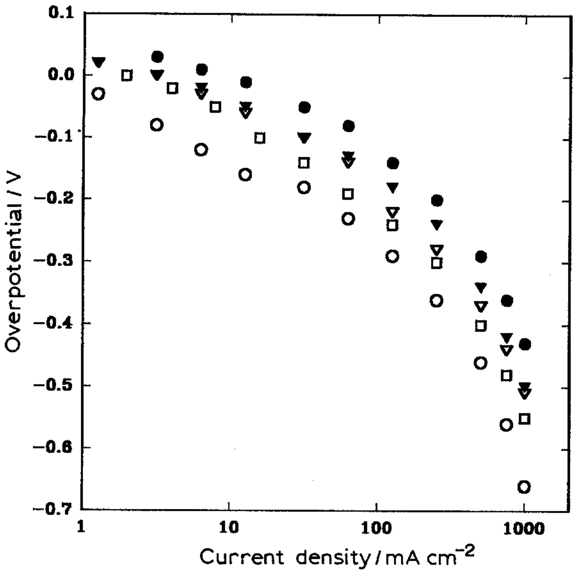

Fig. 6. Cathodic polarization curves for the h.e.r. obtained under galvanostatic conditions in 1 M H_2SO_4 at 298 K on electrodeposited nickel with various concentrations of $PW_{12}O_{40}^{3-}$ and 6.4×10^{-4} M of Cu^{2+}: (○) Ni(Cu); (●) NiCu(PW_{12})10^{-6}; (△) NiCu(PW_{12})10^{-5}; (▲) NiCu(PW_{12})10^{-4}; (□) NiCu(PW_{12})10^{-3}.

−500 mA cm^{-2}. However, the improvement in i_o and η with an increase in [$PW_{12}O_{40}^{3-}$] observed in a basic medium is less significant than that observed on the same electrodes in an acidic medium (see Tables 3 and 4). It may be also noted that the Tafel slopes observed in the basic medium are close to those observed for the same electrodes in the acidic medium (see Table 3).

3.3. Effect of the chemical bath on i_o, b and η

The electrocatalytic activity for the h.e.r. in 1 M H_2SO_4 on electrodeposited nickel from acetate, chloride and sulfate baths containing 6.4×10^{-4} M of Cu^{2+} and 1.0×10^{-4} M of $PW_{12}O_{40}^{3-}$ was investigated. This electrode was labelled NiCu(PW_{12})10^{-4}. Figure 9 shows the cathodic polarization curves obtained in 1 M H_2SO_4 for the NiCu(PW_{12})10^{-4} electrode deposited from these different baths. The kinetic parameters evaluated from Fig. 9 are listed in Table 5. The highest exchange current density and the lowest overpotential were obtained for the NiCu(PW_{12})10^{-4} electrode deposited from the chloride bath, corresponding to the maximum value of [W] on the electrode surface. Consequently, the electrodeposited nickel from the chloride bath is a better electrocatalyst for the h.e.r. in 1 M H_2SO_4 than that deposited from an acetate or sulphate bath. On the other hand, Tafel slope (135 ± 10 mV dec^{-1}) of these electrodeposits does not change with the chemical composition of the bath.

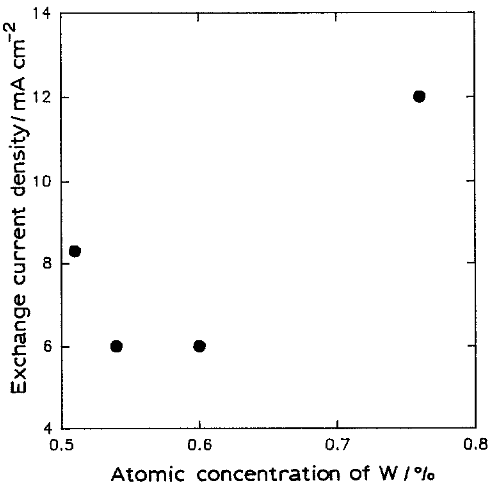

Fig. 7. Variation in exchange current density i_o as a function of [W].

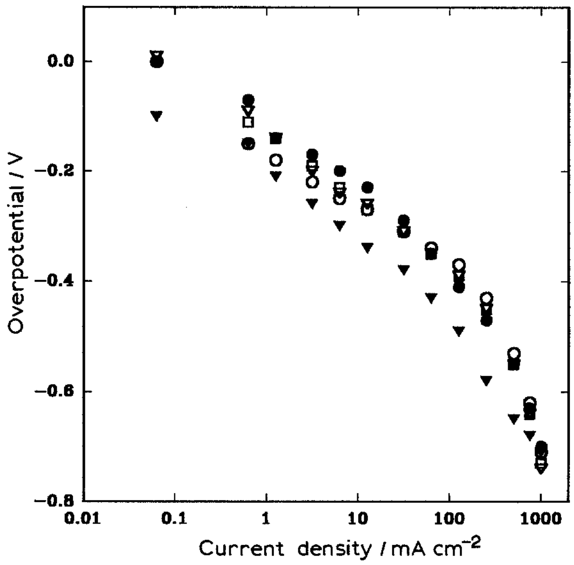

Fig. 8. Cathodic polarization curves for the h.e.r. obtained under galvanostatic conditions in 3 M KOH on nickel electrodeposited with various concentrations of $PW_{12}O_{40}^{3-}$ and 6.4×10^{-4} of Cu^{2+} ions: (○) Ni(Cu); (●) NiCu(PW_{12})10^{-6}; (△) NiCu(PW_{12})10^{-5}; (▲) NiCu(PW_{12})10^{-4}; (□) NiCu(PW_{12})10^{-3}.

4. Conclusion

The hydrogen evolution reaction in an acidic or basic medium on the nickel electrodeposited with Cu^{2+} and

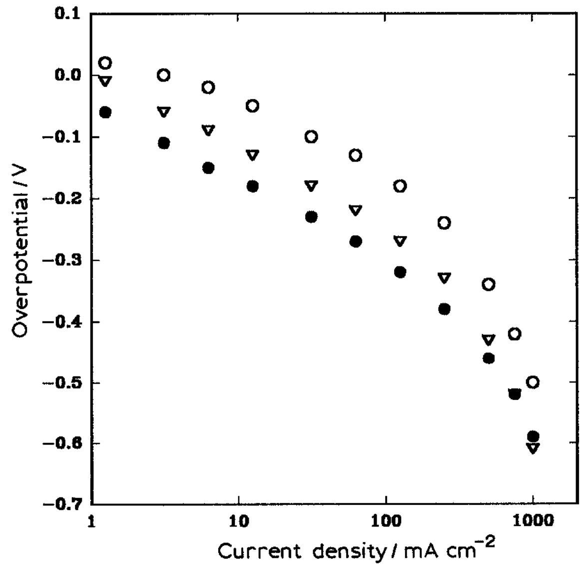

Fig. 9. Cathodic polarization curves for the h.e.r. obtained under galvanostatic conditions in 1 M H_2SO_4 on electrodeposited nickel with 1.0×10^{-4} M of $PW_{12}O_{40}^{3-}$ and 6.4×10^{-4} of Cu^{2+} from chloride, acetate and sulphate baths. (○) chloride, (●) sulphate and (▽) acetate.

Table 5. Variation in the electrocatalytic parameters for the h.e.r. on electrodeposited nickel with 6.4×10^{-4} M *of* Cu^{2+} *and* 1.0×10^{-4} M *of* $PW_{12}O_{40}^{3-}$ *from various chemical baths.*

Chemical bath	$b/mV\,dec^{-1}$	$i_0/mA\,cm^{-2}$	$\lvert\eta\rvert/mV$	*% [Cu]*	*% [W]*
Chloride	130	6.00	300	3.53	0.54
Acetate	140	1.50	430	3.52	0.47
Sulfate	140	0.50	510	3.52	0.32

$PW_{12}O_{40}^{3-}$ was studied. From the results obtained here, it may be concluded that:

(i) The electrocatalytic parameters for the h.e.r. ($i_0$and η) are improved for the electrodes deposited with Cu^{2+} or $PW_{12}O_{40}^{3-}$, or both, with respect to those deposited without Cu^{2+} or $PW_{12}O_{40}^{3-}$, or both.

(ii) The chemical composition of these electrode surfaces has been analysed by X-ray photoelectron spectroscopy and the electrocatalytic properties correlated to the surface species. It was shown that the variation in the electrocatalytic parameters depends only on the quantity of tungsten.

(iii) The h.e.r. exchange current density and the hydrogen overpotential were shown to be improved when [W] increases.

(iv) The improvement in electrocatalytic activity was attributed to a significant increase in i_0 and a decrease in η, and not to a change in the value of b, which remains constant for the different electrodes.

References

[1] O. Savadogo, *Can. J. Chem.* **67** (1989) 382.

[2] O. Savadogo and S. Levesque, *J. Appl. Electrochem.* **21** (1991) 73.

[3] M. M. Jaksic, *Mater. Chem. Phys.*, **22** (1989) 1.

[4] *Idem*, *Int. J. Hydrogen Energy* **12** (1987) 727.

[5] *Idem*, *J. Mol. Catalysis* **38** (1986) 161.

[6] *Idem*, *Electrochem.* **29** (1984) 1539.

[7] N. Alonso-Vanté, B. Schubert and H. Tributsch, *Mat. Chem. Phys.* **22** (1989) 281.

[8] O. Savadogo, *Int. J. Hydrogen Energy* **14** (1989) 865.

[9] O. Savadogo and D. L. Piron, *ibid.* **15** (1990) 715.

[10] O. Savadogo and C. Allard, *J. Appl. Electrochem.* **21** (1991) 73.

[11] O Savadogo and C. Allard, *Can. Met. Quar.* **29** (1990) 285.

[12] K. Amuzgar and O. Savadogo, *J. Appl. Electrochem.* **22** (1992) 166.

[13] J. O'M. Bockris and S. Srinivassan, *in* 'Fuel cells: their electrochemistry', McGraw Hill, New York (1969), Ch. 6, p. 289–350.

[14] R. De Levie, *Electrochem. Acta* **10** (1963) 761.

[15] H. Alenu and K. Juttner, *Electrochem. Acta* **33** (1988) 1101.

[16] R. J. Colton and J. Wayne Rabelais, *Inorganic Chemistry* **15** (1976) 236.